# Inhibition of Angiogenesis by the Antiepidermal Growth Factor Receptor Antibody ImClone C225 in Androgen-independent Prostate Cancer Growing Orthotopically in Nude Mice[1]

**Takashi Karashima, Paul Sweeney, Joel W. Slaton, Sun J. Kim, Daniel Kedar, Jonathan I. Izawa, Zhen Fan, Curtis Pettaway, Daniel J. Hicklin, Taro Shuin, and Colin P. N. Dinney[2]**

Departments of Cancer Biology [T. K., P. S., J. W. S., S. J. K., D. K., J. I. I., C. P. N. D.] and Urology [C. P., C. P. N. D.], Department of Clinical Investigation, Division of Medicine [Z. F.], The University of Texas M. D. Anderson Cancer Center, Houston, Texas 77030; ImClone Systems, New York, New York [D. J. H.]; and Department of Urology, Kochi Medical School, Nankoku, Japan [T. S.]

## ABSTRACT

**In human androgen-independent prostate cancer (PCa), epidermal growth factor receptor (EGFR) regulates angiogenesis, tumor growth, and progression. In this study, we evaluated whether the blockade of EGFR by the anti-EGFR antibody ImClone C225 (IMC-C225) inhibited tumor growth and metastasis by inhibiting angiogenesis, and whether paclitaxel enhanced the results of therapy in androgen-independent PCa. PC-3M-LN4 PCa cells were implanted orthotopically in athymic nude mice and treated with i.p. IMC-C225 (1 mg twice a week) and/or paclitaxel (200 μg once a week). *In vitro* treatment of PC-3M-LN4 with IMC-C225 inhibited EGFR autophosphorylation without any significant antiproliferative effect. In contrast, *in vivo* therapy with IMC-C225 alone ($P < 0.05$) or in combination with paclitaxel ($P < 0.005$) significantly inhibited PCa growth and metastasis. Serum levels of interleukin (IL) 8 were lower after therapy, and IL-8 mRNA expression was down-regulated within the tumors after therapy. The down-regulation of IL-8 correlated with reduced microvessel density. IMC-C225 reduced tumor cell proliferation, enhanced $p27^{kip1}$ expression, and induced tumor and endothelial cell apoptosis. These studies indicate that IMC-C225 has significant antitumor effect in this murine model, mediated in part by inhibition of cellular proliferation and angiogenesis, and by enhancement of apoptosis. The simultaneous administration of paclitaxel enhanced this effect.**

## INTRODUCTION

Despite increased public awareness and significant progress in early diagnosis and improved treatment modalities in recent years, adenocarcinoma of the prostate remains one of the leading causes of cancer-related deaths in North American men (1). Currently, patients with locally advanced or metastatic PCa[3] are treated by androgen deprivation alone or in combination with local therapy (2). Although most of these patients initially respond to androgen ablation, the majority will subsequently have disease progression and die of metastatic androgen-independent PCa. Empiricism in the treatment of PCa is unlikely to produce significant improvement over current therapy, and, hence, innovative therapies that target androgen-independent PCa must be developed if we are to improve the prognosis of these patients (3, 4).

PCa is regulated by the mitogenic effects of several polypeptide growth factors, including IGF-1, the fibroblast growth factors, platelet-derived growth factor, EGF, and TGF-α (5–11). High levels of IGF-1 have been shown recently to be associated with an increased risk for PCa (12). Several autocrine and paracrine loops involving the EGFR and its ligands, EGF and TGF-α, are also postulated to stimulate the growth of prostate epithelial and stromal cells independent of the activity of androgens (5, 13). These pathways become much more essential to PCa growth once androgen insensitivity has emerged (5, 13). Furthermore, EGFR signaling pathways may also be involved in PCa invasion and angiogenesis, both of which are crucial for progression and metastasis (14–17). Novel therapies that target androgen-dependent and -independent proliferation, as well as invasion and angiogenesis may have enormous potential for improving the care of patients with advanced PCa (18–20).

The anti-EGFR MAb IMC-C225 binds to the EGFR with high affinity and inhibits activation of receptor tyrosine kinase activity (21–25). This antibody inhibits the *in vitro* proliferation

Received 8/31/01; revised 2/12/02; accepted 2/13/02.
The costs of publication of this article were defrayed in part by the payment of page charges. This article must therefore be hereby marked *advertisement* in accordance with 18 U.S.C. Section 1734 solely to indicate this fact.
[1] Supported by NIH Grant CA67914, National Cancer Institute Cancer Center Core Grant CA16671, NIH Prostate Specialized Programs of Research Excellence Grant P50-CA90270-01, and a grant from ImClone Systems.
[2] To whom requests for reprints should be addressed, at Department of Urology, Box 446, The University of Texas M. D. Anderson Cancer Center, 1515 Holcombe Boulevard, Houston, TX 77030. Phone: (713) 792-3250; Fax: (713) 792-4824. E-mail: cdinney@mdanderson.org.

[3] The abbreviations used are: PCa, prostate cancer; MAb, monoclonal antibody; EGF, epidermal growth factor; IGF, insulin-like growth factor; EGFR, epidermal growth factor receptor; bFGF, basic fibroblast growth factor; VEGF, vascular endothelial cell growth factor; IL-8, interleukin-8; MMP-9, matrix metalloproteinase type 9; CDK, cyclin-dependent kinase; PCNA, proliferating cell nuclear antigen; TUNEL, terminal deoxynucleotidyl transferase (Tdt)-mediated nick end labeling; TGF, transforming growth factor; MAPK, mitogen-activated protein kinase; poly(dT), polydeoxythymidylic acid; MTT, 3-(4,5-dimethylthiazol-2-ly)-2,5-diphenyltetrazolium bromide; MVD, microvessel density.

of a variety of tumor cells and human xenografts growing in athymic nude mice (26–32). We reported recently that treatment of human transitional cell carcinoma with IMC-C225 inhibited tumor growth and metastasis in a murine model by inhibiting angiogenesis (33). IMC-C225 inhibited tumor-induced neovascularization by down-regulating the expression of the angiogenic factors VEGF, IL-8, bFGF, and MMP-9 (33, 34). Moreover, paclitaxel synergistically enhanced the antiangiogenic effect of IMC-C225 (34).

EGFR blockade has been evaluated as therapy for PCa (32, 35, 36). IMC-C225 inhibited the proliferation of the androgen-independent PCa cell lines DU145 and PC3 (35–40). The antibody-induced growth inhibition of DU145 was associated with induction of the CDK inhibitor, $p27^{kip1}$ (37). Treatment of DU145 xenografts, which express relatively high levels of the EGFR, with IMC-C225 and doxorubicin induced the regression of established s.c. tumors (32). Recently, multiagent chemotherapy regimens including paclitaxel have effectively treated human PCa (3, 9, 41, 42). Because PCa growth and metastasis are regulated by tumor host interactions within the prostate, we evaluated the therapeutic effect of IMC-C225 and paclitaxel against highly metastatic androgen-independent PCa growing within the prostate of athymic nude mice (43).

## MATERIALS AND METHODS

**Cell Lines and Culture Conditions.** Cells of the highly metastatic human androgen-independent prostate carcinoma line PC-3M-LN4 were grown as monolayer cultures in RPMI 1640 supplemented with 10% fetal bovine serum, vitamins, sodium pyruvate, L-glutamine, nonessential amino acids, and penicillin-streptomycin (complete RPMI) as described previously (43).

**Reagents.** Chimeric anti-EGFR IMC-C225 was generously provided by ImClone Systems, Inc. (New York, NY). Paclitaxel was purchased from Bristol-Myers Squibb Co. (Princeton, NJ).

***In Vitro* Growth Inhibition.** *In vitro* antiproliferation was determined after incubating $1 \times 10^4$ PC-3M-LN4 cells for 24 h in 10% fetal bovine serum-supplemented MEM, then exchanging the medium for serum-free medium containing EGF (40 ng/ml; R & D Systems Inc., Minneapolis, MN) and up to 100 μg/ml IMC-C225 with or without paclitaxel. Viable cells were counted by MTT assay (44).

**Western Immunoblotting and Immunoprecipitation.** Cells were lysed in NP40 lysis buffer [50 mM Tris-HCl (pH 7.4), 150 mM NaCl, 0.5% NP40, 50 mM NaF, 1 mM Na3VO4, 1 mM phenylmethylsulfonyl fluoride, 25 μg/ml leupeptin, and 25 μg/ml aprotinin) at 4°C. The supernatants were cleared by centrifugation. Protein concentrations were measured by the Bradford method. Equal amounts of protein were subjected to immunoprecipitation in the presence of mouse antihuman EGFR antibody (Oncogene Research Products, Boston, MA) for 2 h at 4°C, followed by incubation with immobilized protein G plus/protein A-agarose beads (Oncogene Research Products) overnight at 4°C. For Western immunoblotting, the immunoprecipitates or equal amounts of crude extract were boiled in Laemmli SDS sample buffer, resolved by SDS-PAGE, transferred to nitrocellulose, and probed with mouse antiphosphorylation primary antibody (Upstate Biotechnology, Lake Placid, NY), rabbit anti-EGFR primary antibody (Upstate Biotechnology), or rabbit anti $p27^{kip1}$ primary antibody (Santa Cruz Biotechnology Inc., Santa Cruz, CA) at 4°C overnight. After the blots were incubated for another 1 h at room temperature with horseradish peroxidase-labeled antimouse secondary antibody (Amersham Life Science Inc., Arlington Heights, IL), signals were detected by using the enhanced chemiluminescence assay (Amersham Life Science Inc.) according to the manufacturer's instructions (40).

**Animals.** Male athymic nude BALB/c mice were obtained from the Animal Production Area of the National Cancer Institute, Frederick Cancer Research Facility (Frederick, MD). The mice were maintained in a laminar airflow cabinet under specific pathogen-free conditions and used at 8–12 weeks of age. All of the facilities were approved by the American Association for Accreditation of Laboratory Animal Care in accordance with the current regulations and standards of the United States Department of Agriculture, the Department of Health and Human Services, and the NIH.

**Orthotopic Implantation of Tumor Cells.** Cultured PC-3M-LN4 cells (60–70% confluent) were prepared for injection as described previously (43). Mice were anesthetized with i.p. nembutol. For orthotopic implantation, a lower midline incision was made, and viable tumor cells ($1 \times 10^6$/0.04 ml) in HBSS were injected beneath the capsule of the prostate. The formation of a bulla indicated a satisfactory injection. The prostate was returned to the abdominal cavity, and the abdominal wall was closed with a single layer of metal clips.

***In Vivo* Therapy of Established Human PCa Growing in the Prostate of Athymic Nude Mice.** Treatment commenced 3 days after tumor implantation. Mice were randomly separated into four groups and treated for 5 weeks. One group was treated with PBS (200 μl i.p.), a second with IMC-C225 (1 mg i.p twice weekly), a third with paclitaxel (10 μg/g i.p, weekly), and a fourth with a combination of IMC-C225 and paclitaxel. Tumors were harvested 5 weeks after initiation of therapy. The primary tumors were removed and weighed, and the presence of lymph node metastases was determined grossly and microscopically. The prostates were then either fixed in 10% buffered formalin, placed in OCT compound (Miles Laboratories, Elkhart, IN), or mechanically dissociated and put into tissue culture. The lymph nodes were either fixed in 10% buffered formalin or mechanically dissociated and put into tissue culture.

**Enzyme-linked Immunosorbent Assay.** Blood was collected from the tail vein of each mouse at necropsy, and the serum was separated by centrifugation. Levels of human bFGF, IL-8, and VEGF proteins were determined using the commercial Quantikine ELISA kit (R & D Systems, Inc.). This kit has minimum cross-reaction with other species.

***In Situ* mRNA Hybridization Analysis.** Specific antisense oligonucleotide DNA probes were designed complementary to the mRNA transcripts based on published reports of the cDNA sequences for MMP-9, VEGF, IL-8, bFGF, and EGFR (45, 46). The specificity of the oligonucleotide sequence was initially determined by a Gene Bank European Molecular Biology Library database search with the use of the Genetics Computer Group sequence analysis program (GCG, Madison, WI) based on the FastA algorithm; these sequences showed 100%

homology with the target gene and minimal homology with nonspecific mammalian gene sequences. The specificity of each sequence was also confirmed by Northern blot analysis (45). A poly(dT)$_{20}$ oligonucleotide was used to verify the integrity and lack of degradation of the mRNA in each sample. All of the DNA probes were synthesized with six biotin molecules (hyperbiotinylated) at the 3′ end via direct coupling with the use of standard phosphoramidite chemistry (Research Genetics, Huntsville, AL). The lyophilized probes were reconstituted to a stock solution at 1 μg/μl in 10 mmol/liter Tris (pH 7.6) and 1 mmol/liter EDTA. Immediately before use, the stock solution was diluted with probe dilution (Research Genetics).

*In situ* mRNA hybridization was performed as described previously with minor modifications (46) using the Microprobe Manual Staining System (Fisher Scientific, Pittsburgh, PA; Refs. 45, 46). Tissue sections (4 mm) of formalin-fixed, paraffin-embedded specimens were mounted on ProbeOn slides (Fisher Scientific). The slides were placed in the Microprobe slide holder, dewaxed, and rehydrated with Auto dewaxer and Auto alcohol (Research Genetics) followed by enzymatic digestion with pepsin. Hybridization of the probe was performed for 45 min at 45°C, and the samples were then washed three times with 2× SSC for 2 min at 45°C. The samples were incubated with alkaline phosphatase-labeled avidin for 30 min at 45°C, rinsed in 50 mM Tris buffer (pH 7.6), rinsed with alkaline phosphatase enhancer for 1 min, and incubated with a chromogen substrate for 15 min at 45°C. Additional incubation with fresh chromogen substrate was done if it was necessary to enhance a weak reaction. A red stain indicated a positive reaction in this assay. To check the specificity of the hybridization signal, the following controls were performed: (*a)* RNase pretreatment of sections; and (*b)* substituting a biotin-labeled sense probe for the antisense probe. No hybridization signal was observed under either of these conditions. Control for endogenous alkaline phosphatase included treatment of the sample in the absence of the biotinylated probe and the use of chromogen alone (45, 46).

**Quantification of Color Reaction.** Stained sections were examined in a Zeiss photomicroscope (Carl Zeiss, Thornwood, NY) equipped with a three-chip, charge-coupled device color camera (model DXC-969 MD; Sony Corp., Tokyo, Japan). The images were analyzed using the Optimas image analysis software (version 4.10; Bothell, WA). The slides were prescreened by one of the investigators to determine the range in staining intensity of the slides to be analyzed. Images covering the range of staining intensities were captured electronically, a color bar (montage) was created, and a threshold value was set in the red, green, and blue mode of the color camera. All of the subsequent images were quantified based on this threshold. The integrated absorbance of the selected fields was determined based on its equivalence to the mean log inverse gray value multiplied by the area of the field. The samples were not counterstained, so the absorbance was attributable solely to the product of the *in situ* hybridization reaction. Three different fields in each sample were quantified to derive an average value. The intensity of staining was determined by comparison with the integrated absorbance of poly(dT)$_{20}$. The results were presented as the ratio of the expression level of each gene compared with controls (defined as 100; Ref. 34).

**Immunohistochemical Analysis.** For immunohistochemical analysis, frozen tissue sections (8-μm thick) were fixed with cold acetone. Tissue sections (5-μm thick) of formalin-fixed, paraffin-embedded specimens were deparaffinized in xylene, rehydrated in graded alcohol, and transferred to PBS. The slides were rinsed twice with PBS, and appropriate antigen retrieval was performed; endogenous peroxidase was blocked by the use of 3% hydrogen peroxide in PBS for 12 min. The samples were washed three times with PBS and incubated for 20 min at room temperature with a protein-blocking solution of PBS (pH 7.5) containing 5% normal horse serum and 1% normal goat serum. Excess blocking solution was drained, and the samples were incubated for 18 h at 4°C with a (1:25) dilution of a rabbit polyclonal anti-IL-8 antibody (Biosource International, Camarillo, CA), a 1:100 dilution of rat monoclonal anti-CD31 antibody (PharMingen, San Diego, CA; 47), a 1:100 dilution of mouse monoclonal anti-PCNA antibody (DAKO, Glostrup, Denmark), or a 1:250 dilution of mouse polyclonal anti p27$^{kip1}$ antibody (Transduction Laboratory, Kingston, MA). The samples were then rinsed four times with PBS and incubated for 60 min at room temperature with the appropriate dilution of the secondary antibody: antirabbit IgG, Fab$_2$ fragment (Jackson ImmunoResearch Laboratory, Inc., West Grove, PA), peroxidase-conjugated antirat IgG (IgG; H+L; Jackson ImmunoResearch Laboratory, Inc.), or antimouse IgG1 (PharMingen). The slides were rinsed with PBS and incubated for 5 min with diaminobenzidine (Research Genetics). The sections were then washed three times with PBS, counterstained with Gill's hematoxylin (Biogenex Laboratories, San Ramon, CA), and washed three times with PBS. The slides were mounted with mounting medium after dehydration with alcohol and xylene (Universal Mount; Research Genetics).

**Quantification of Intensity of Immunostaining.** The intensity of immunostaining of IL-8 was quantified in each sample by an image analyzer using the Optimas software program (Bioscan, Edmonds, WA). Five different areas in each sample were evaluated to yield an average measurement of intensity of immunostaining. The results were presented as a ratio between the expression by the tumor and normal mucosa (which was set at 100; Ref. 34).

**Quantification of MVD.** MVD was determined by light microscopy after immunostaining of sections with anti-CD31 antibodies according to the procedure of Weidner *et al.* (48). Clusters of stained endothelial cells distinct from adjacent microvessels, tumor cells, or other stromal cells were counted as one microvessel. Tissue images were recorded using a cooled CCD Optotronics Tec 470 camera (Optotronics Engineering, Goletha, CA) linked to a computer and digital printer (Sony Corporation). The MVD was expressed as the average number of five highest areas identified within a single ×100 field.

**Quantification of Cell Proliferation, p27$^{kip1}$, and Apoptosis.** Cell proliferation, p27$^{kip1}$ expression, and apoptosis were determined by immunohistochemical staining of tissue sections with anti-PCNA and anti-p27$^{kip1}$ antibodies and TUNEL assay. Tissue images were recorded using a cooled CCD Optotronics Tec 470 camera (Optotronics Engineering) as before. Densities of proliferative cells and apoptotic cells were expressed as the mean for the five highest areas identified within a single ×100 field (34).

**TUNEL Assay.** For the TUNEL assay, tissue sections (5-μm thick) of formalin-fixed, paraffin-embedded specimens were deparaffinized in xylene, rehydrated in graded alcohol, and transferred to PBS. The slides were rinsed twice with distilled water with BRIJ and treated with proteinase K (20 μg/ml) for 15 min; endogenous peroxidase was blocked by use of 3% hydrogen peroxide in PBS for 12 min. The samples were washed three times with distilled water with BRIJ and incubated for 10 min at room temperature with Tdt buffer. Excess Tdt buffer was drained, and the samples were incubated for 18 h at 4°C with terminal transferase and biotin-16-dUTP. The samples were then rinsed four times with termination buffer (300 mM sodium chloride, 30 mM sodium citrate) and incubated for 30 min at 37°C with a 1:400 dilution of peroxidase-conjugated streptavidin. The slides were rinsed with PBS and incubated for 5 min with diaminobenzidine (Research Genetics). The sections were then washed three times with PBS, counterstained with Gill's hematoxylin (Biogenex Laboratories), washed three times with PBS, and mounted with a mounting medium (Universal Mount; Research Genetics) after dehydration with alcohol and xylene (34).

**Immunofluorescence Double Staining of Tumor and Endothelial Cells.** Frozen tissue sections (8 μm) were fixed with cold acetone for 5 min, with acetone plus chloroform (1:1) for 5 min, and with acetone for 5 min. The samples were washed three times with PBS and incubated with protein-blocking solution containing 5% normal horse serum and 1% normal goat serum in PBS for 20 min. The blocking solution was drained, and the samples were incubated with a 1:400 dilution of rat monoclonal anti-CD31 antibody (PharMingen; Ref. 47) for 24 h at 4°C. The samples were then rinsed with PBS three times for 3 min and incubated with protein-blocking solution for 10 min at room temperature. The blocking solution was drained, and the samples were incubated with a 1:200 dilution of secondary goat antirat conjugated to Texas Red (Jackson ImmunoResearch Laboratory) for 1 h at room temperature. The samples were then washed two times with PBS containing 0.1% BRIJ and then washed with PBS for 5 min. TUNEL was performed using a commercial kit (Promega, Madison, WI) with the following modifications. The samples were fixed with 4% paraformaldehyde for 10 min at room temperature. The samples were washed with PBS two times for 5 min and then incubated with 0.2% Triton X-100 for 15 min at room temperature. The samples were then washed with PBS two times for 5 min each and incubated with equilibration buffer (from kit) for 10 min at room temperature. The equilibration buffer was drained, and reaction buffer containing equilibration buffer, nucleotide mix, and Tdt enzyme was added to the tissue sections and incubated in a humid atmosphere at 37°C for 1 h avoiding exposure to light. To terminate the reaction, the samples were immersed in 2× SSC for 15 min. The samples were then washed three times for 5 min to remove unincorporated fluorescein-dUTP.

To quantify endothelial cells, the samples were incubated with 300 g/ml of Hoechst stain for 10 min at room temperature. This medium stains all of the cell nuclei blue. The samples were then washed with PBS two times for 5 min each. To preserve fluorescence and reduce bleaching, the Prolong antifade kit (Molecular Probes, Inc., Eugene, OR) was used to mount coverslips. The slides were examined using a fluorescent microscope (Inverted System IX70; Olympus, Melville, NY). Endothelial cells were identified by red fluorescence at 600 nm, and DNA fragmentation was detected by localized green fluorescence within the nucleus of apoptotic cells at 520 nm, and colocalized yellow fluorescence within the nucleus indicated apoptotic endothelial cells. Results were expressed as an average of the ratio of apoptotic endothelial cells (yellow nuclei) to the total number of nucleus of endothelial cells (red with blue nuclei) in 10 random fields at ×100 magnification (34).

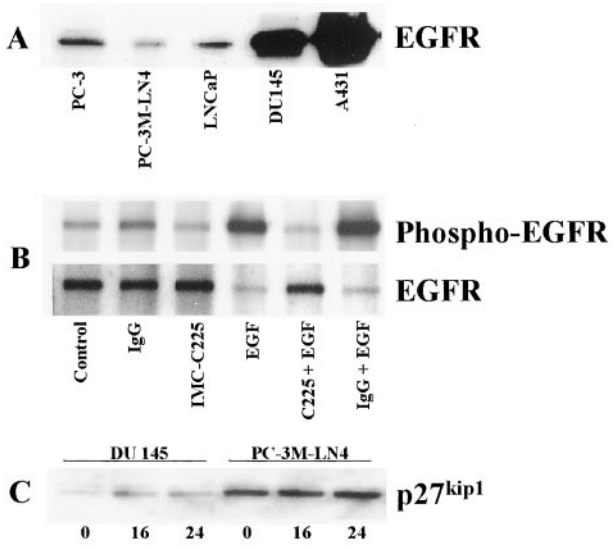


*Fig. 1* The EGFR expression level of several PCa cells was evaluated by Western immunoblotting. PC-3 M-LN4 cells expressed the lowest level of EGFR compared with other cells (*A*). IMC-C225 inhibited EGFR tyrosine kinase autophosphorylation of PC-3 M-LN4 cells. Cells were immunoprecipitated with anti-EGFR antibody after treatment with 10 μg/ml of IMC-C225 in the presence or absence of EGF 40 ng/ml and then resolved by SDS-PAGE. IMC-C225 significantly inhibited EGFR tyrosine phosphorylation in response to exogenous EGF stimulation. Nonphosphorylated EGFR expression was decreased by exogenous EGF with or without antihuman nonspecific IgG (10 μg/ml; *B*). $p27^{kip1}$ expression in DU145 and PC-3 M-LN4 cells was determined by Western immunoblotting. IMC-C225 therapy increased $p27^{kip1}$ expression after 16 and 24 h in DU145 cells. In contrast, IMC-C225 did not alter $p27^{kip1}$ expression in PC-3 M-LN4 cells (*C*).

**Statistical Analysis.** Tumor weights and staining intensities are expressed as median + SD. Differences among the treatment groups in the number of vessels, proliferative cells, and apoptotic cells, and in the staining intensity for EGFR and bFGF, VEGF, IL-8, and MMP-9 within the prostate tumors were statistically analyzed using the Mann-Whitney test. Incidences of tumors and metastases were analyzed by the $\chi^2$ test. Differences with $P < 0.05$ were considered significant.

## RESULTS

**Inhibition of Ligand-stimulated EGFR Tyrosine Phosphorylation in PC-3M-LN4.** We first determined EGFR expression level of PCa cells (PC-3, PC-3M-LN4, LNCaP, and DU145) and A431 as positive control. PC-3M-LN4 cells expressed the lowest level of EGFR compared with other cells (Fig. 1*A*). Next, we determined whether IMC-C225 inhibits

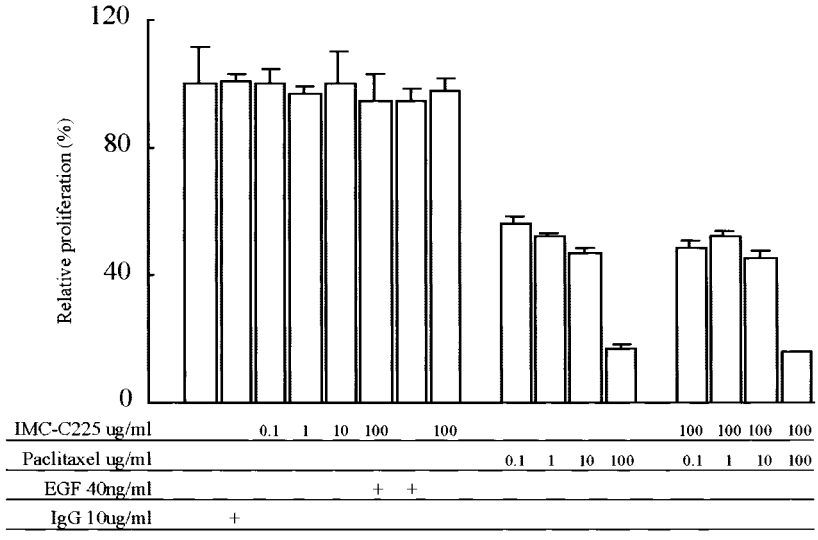


*Fig. 2 In vitro* cellular proliferation of PC-3 M-LN4 cells after therapy with IMC-C225 and paclitaxel as measured by the MTT assay. After EGF (40 ng/ml) stimulation, IMC-C225 had no significant antiproliferative effect on the PC-3 M-LN4 cells compared with untreated controls. A dose-dependent antiproliferative effect was noted with paclitaxel. IMC-C225 did not potentiate the antiproliferate effects of paclitaxel; *bars*, ±SD.

EGF-stimulated tyrosine phosphorylation of the EGFR in PC-3M-LN4 cells. Under basal conditions in serum-free medium, PC-3M-LN4 cells demonstrated a low level of EGFR tyrosine autophosphorylation, which was enhanced after exposure to EGF for 15 min. IMC-C225 (10 μg/ml) significantly inhibited the EGFR tyrosine phosphorylation ($M_r$ 170,000 band) by PC-3M-LN4 cells in response to exogenous EGF stimulation (Fig. 1*B*). Fig. 1*C* shows induction of CDK inhibitor $p27^{kip1}$ in DU145 and PC-3M-LN4 treated with IMC-C225 for 16 and 24 h. As reported previously, IMC-C225 increased $p27^{kip1}$ expression in DU145 cells after 16-h exposure to IMC-C225 (49). However, the $p27^{kip1}$ expression in PC-3M-LN4 cells was unaltered by IMC-C225 treatment.

**Inhibition of *in Vitro* Proliferation by IMC-C225 and Paclitaxel.** We next evaluated the *in vitro* antiproliferative effects of IMC-C225 treatment of PC-3M-LN4 cells. After exposure to EGF, treatment with up to 100 μg of IMC-C225 failed to significantly inhibit the growth of PC-3M-LN4 cells as measured by the MTT assay (Ref. 44; Fig. 2). Moreover, IMC-C225 did not enhance the *in vitro* antiproliferative effects of paclitaxel.

**Inhibition of Growth and Metastasis of Human PCa.** The purpose of these experiments was to determine whether IMC-C225 would inhibit the growth and metastasis of PC-3M-LN4 tumor cells growing within the prostate of athymic nude mice and whether this effect was enhanced by paclitaxel. Therapy commenced 3 days after tumor implantation and continued for 5 weeks, at which point all of the control mice had become moribund and had to be sacrificed. Treated mice were closely monitored for any signs of progressive disease and were euthanized if they became moribund before 5 weeks of therapy was completed. The results of therapy are summarized in Table 1. Each therapy effectively inhibited tumor size compared with the control group ($P < 0.05$). In particular, combination therapy with IMC-C225 and paclitaxel (median tumor weight 181 mg) was significantly more effective than control saline therapy (median tumor weight 672 mg; $P < 0.005$**)**. Furthermore, the number of mice with grossly detectable spontaneous lymph node metastases >5 mm in size (1 of 7) was lower in the group that received combination treatment compared with control mice (5 of 6), mice receiving paclitaxel alone (5 of 7), or mice receiving IMC-C225 alone (6 of 9; $P < 0.05$).

**Inhibition of Serum IL-8 by IMC-C225 and Paclitaxel.** Serum concentrations of IL-8 and bFGF were measured by ELISA after therapy with IMC-C225 and paclitaxel (Table 2). Serum IL-8 levels were decreased by 50% after therapy with either IMC-C225 or paclitaxel. IMC-C225 and paclitaxel together reduced IL-8 by 90%. Serum bFGF levels were not significantly altered by therapy. VEGF was not detectable in the serum of mice bearing PC-3M-LN4 tumors.

**Down-Regulation of IL-8 Expression after Therapy with IMC-C225 and Paclitaxel.** The mRNA expression of bFGF, VEGF, IL-8, MMP-9, and EGFR was determined by *in situ* hybridization. (Table 3). IL-8 mRNA expression was significantly lower within the tumors of mice treated with IMC-C225 alone or in combination with paclitaxel compared with saline-treated controls ($P < 0.05$, Fig. 3, Table 3). Expression of bFGF, VEGF, MMP-9, and EGFR mRNA were unaltered by therapy. The change in IL-8 mRNA levels was mirrored by decreases in IL-8 protein expression in IMC-C225 and combination therapy tumors ($P < 0.05$, Fig. 3; Table 3).

**Enhancement of Apoptosis, Up-Regulation of $p27^{kip1}$ Expression, and Inhibition of Proliferation and MVD by Treatment with IMC-C225 and Paclitaxel.** We evaluated the effect of therapy with IMC-C225 and paclitaxel on cellular proliferation, MVD, and apoptosis of tumor and endothelial cells (Table 4; Fig. 4). The number of PCNA-positive cancer cells counted per ×100 field was significantly decreased from 244 ± 55 in saline-treated control mice to 164 ± 35 and 174 ± 43 after therapy with IMC-C225 alone and paclitaxel alone, respectively. Treatment with IMC-C225 and paclitaxel in combination significantly inhibited proliferation (139 ± 33 PCNA-positive cells) compared with controls or either therapy alone ($P < 0.05$; Table 4). The number of apoptotic cancer cells counted per ×100 field increased from 15 ± 4 in controls to 24 ± 9, 29 ± 8, and 30 ± 9 after therapy with IMC-C225,

*Table 1* Results of therapy with IMC-C225 and/or paclitaxel for human prostate cancer (PC-3M-LN4) growing orthotopically in athymic nude mice

Mice were implanted with $1 \times 10^6$ cells, and treatment commenced 3 days later. Mice were randomly separated into four groups. All mice were sacrificed 5 weeks after initiation of therapy. *In vivo* IMC-C225 and paclitaxel significantly inhibited the tumor growth of PC-3M-LN4 ($P < 0.05$). Combination therapy with IMC-C225 and paclitaxel was the most effective for inhibiting prostate tumor growth ($P < 0.005$) and metastasis ($P < 0.05$).

| Therapy | Incidence | Tumorigenicity median (mg) | Range (mg) | Lymph node met > 5 mm |
|---|---|---|---|---|
| Control (saline) | 8/8 | 672 | 238–1608 | 5/6 |
| IMC-C225 | 9/9 | 352[a] | 96–644 | 6/9 |
| Paclitaxel | 9/9 | 416[a] | 110–828 | 5/7 |
| IMC-C225/ paclitaxel | 9/9 | 181[b] | 48–540 | 1/7[c] |

[a] $P < 0.05$.
[b] $P < 0.005$ against control ($P$: Mann-Whitney $U$ test).
[c] $P < 0.05$ against control, IMC-C225 and paclitaxel (p: chi-square test).

*Table 2* Serum protein production of human bFGF and IL-8 after therapy with IMC-C225 and/or paclitaxel

Serum was collected from mice tail vein just before sacrifice, and human bFGF and IL-8 protein production was measured using ELISA. IL-8 protein expression was significantly reduced by therapy with either paclitaxel or combination compared with controls ($P < 0.05$). Moreover, the combination therapy with IMC-C225 and paclitaxel significantly decreased IL-8 protein compared with paclitaxel ($P < 0.05$).

| | Serum protein production | |
|---|---|---|
| Therapy | Human bFGF (pg/ml) | Human IL-8 (pg/ml) |
| Control (saline) | 284 ± 151 | 406 ± 290 |
| IMC-C225 | 194 ± 52 | 168 ± 255 |
| Paclitaxel | 175 ± 101 | 202 ± 147[a] |
| IMC-C225/paclitaxel | 410 ± 47 | 28 ± 18[a,b] |

[a] $P < 0.05$ against control.
[b] $P < 0.05$ against paclitaxel ($P$: Mann-Whitney $U$ test) (±SD)

paclitaxel, and IMC-C225 plus paclitaxel, respectively ($P < 0.05$; Table 4). We also observed an increase in $p27^{kip1}$ expression after therapy with IMC-C225 alone (18 ± 5) or in combination with paclitaxel (23 ± 11), compared with paclitaxel (10 ± 5) or saline (9 ± 4) ($P < 0.05$).

Because therapy with IMC-C225 inhibited IL-8 expression, we determined whether IMC-C225 alone or in combination with paclitaxel inhibits angiogenesis *in vivo*. MVD was significantly decreased in mice treated with IMC-C225 alone or in combination with paclitaxel compared with control group ($P < 0.05$; Fig. 4; Table 4). Paclitaxel alone had no effect on MVD and did not enhance the reduction in MVD observed after IMC-C225 therapy.

Endothelial cell apoptosis was determined by double-labeled immunofluorescence. By this technique, endothelial cells fluoresce red, whereas green fluorescence is detected within the nuclei of apoptotic cells. Double labeling of endothelial cells undergoing apoptosis results in localized yellow fluorescence. The endothelial cell apoptotic index was calculated as the ratio of double labeled to total nuclei of endothelial cells counted per ×100 field. Treatment with either IMC-C225 alone or IMC-C225 plus paclitaxel significantly increased the apoptotic index of endothelial cells to 0.88 ± 0.18 and 1.36 ± 0.57, respectively, compared with treatment with paclitaxel alone (0.28 ± 0.21) or saline (0.13 ± 0.26; $P < 0.05$; Table 4; Fig. 4).

## DISCUSSION

Whereas advanced PCa initially responds to hormone deprivation therapy, most patients will eventually develop androgen-independent cancer, rendering additional hormonal manipulation relatively ineffective (2, 3). This hormone-independent disease state is characterized by an inhibition of apoptosis within the tumor after androgen deprivation (47). The progression from androgen-dependent to androgen-independent disease is associated with the up-regulation of autocrine or paracrine loops involving several polypeptide growth factors including EGF, TGF-α, and IGF (5, 6, 8, 11). In androgen-insensitive DU145 cells, for instance, there is an elevated basal activity of MAPK (35), which is a downstream target of the EGFR-mediated signal transduction pathway. The elevated basal level of MAPK can be abrogated by blockade of the EGF receptor kinase with the selective EGFR tyrosine kinase inhibitor tyrphosin AG1478 (35), and tumor growth can be inhibited by the anti-EGFR antibody IMC-C225 or by anti-TGF-α oligonucleotides (37–40, 50). A recent clinical study indicated that PCa progression is characterized by a transition from a paracrine to an autocrine loop between the EGFR and TGF-α; in primary tumors, the neoplastic cells express EGFR and the surrounding stromal cells express TGF-α, whereas in advanced disease, the neoplastic cells coexpress the EGFR and TGF-α (51, 52). Another recent clinical study (53) examined the activation status of MAPK in primary and metastatic human prostate tumor specimens and reported that non-neoplastic prostate tissue has little or no MAPK activity. However, in prostate tumors, the level of activated MAPK increased with increasing Gleason score and tumor stage. Two patients in their study originally showed no activation of MAPK in tumor samples before androgen ablation therapy but exhibited high levels of activated MAPK in their recurrent tumors after androgen ablation treatment (53). Taken together, these results indicate that during PCa progression after androgen ablation therapy, there may be a microenvironment in which peptide growth factors activate signal transduction pathways that help to drive PCa cells to an androgen-independent state.

Even in the androgen-responsive state of PCa, androgens may mediate their stimulatory effects on prostate cells partially through an autocrine or paracrine loop involving TGF-α and the EGFR (54–56). Exposure of the androgen-responsive prostate carcinoma cell line ALVA101 to testosterone or to its active metabolite dihydrotestosterone up-regulated both TGF-α and the EGF receptor at the mRNA level and increased cellular proliferation. An anti-EGFR MAb, 528, blocked the cell proliferation induced by dihydrotestosterone (55). On the other hand, growth factors such as EGF or IGF-1 may stimulate androgen receptor-mediated gene transcription in the absence of androgen

*Table 3* In vivo mRNA and protein expression after therapy with IMC-C225 and/or paclitaxel

mRNA and protein expression of IL-8 was reduced in tumors treated with either IMC-C225 alone and combination with paclitaxel. mRNA levels for bFGF, VEGF, MMP-9, and EGFR remained unaltered in the different treatment groups.

| | mRNA expression index[a] | | | | | Protein expression index[b] |
|---|---|---|---|---|---|---|
| Therapy | bFGF | VEGF | IL-8 | MMP-9 | EGFR | IL-8 |
| Control (saline) | 100 | 100 | 100 | 100 | 100 | 100 |
| IMC-C225 | 98 | 104 | 72[c,d] | 95 | 98 | 75[c,d] |
| Paclitaxel | 97 | 92 | 112 | 84 | 110 | 108 |
| IMC-C225/paclitaxel | 115 | 101 | 68[c,d] | 98 | 106 | 64[c,d] |

[a] The intensity of the cytoplasmic color reaction was quantified by an image analyzer and compared with the maximal intensity of poly (dT) color reaction in each sample. The results were presented as a number for each group compared with controls defined as 100.

[b] The intensity of the cytoplasmic immunostaining was quantified by an image analyzer in five different areas of each sample to yield an average measurement, which was compared with the intensity of the saline controls defined as 100.

[c] $P < 0.05$ against control.

[d] $P < 0.05$ against paclitaxel ($P$: Mann-Whitney $U$ test).

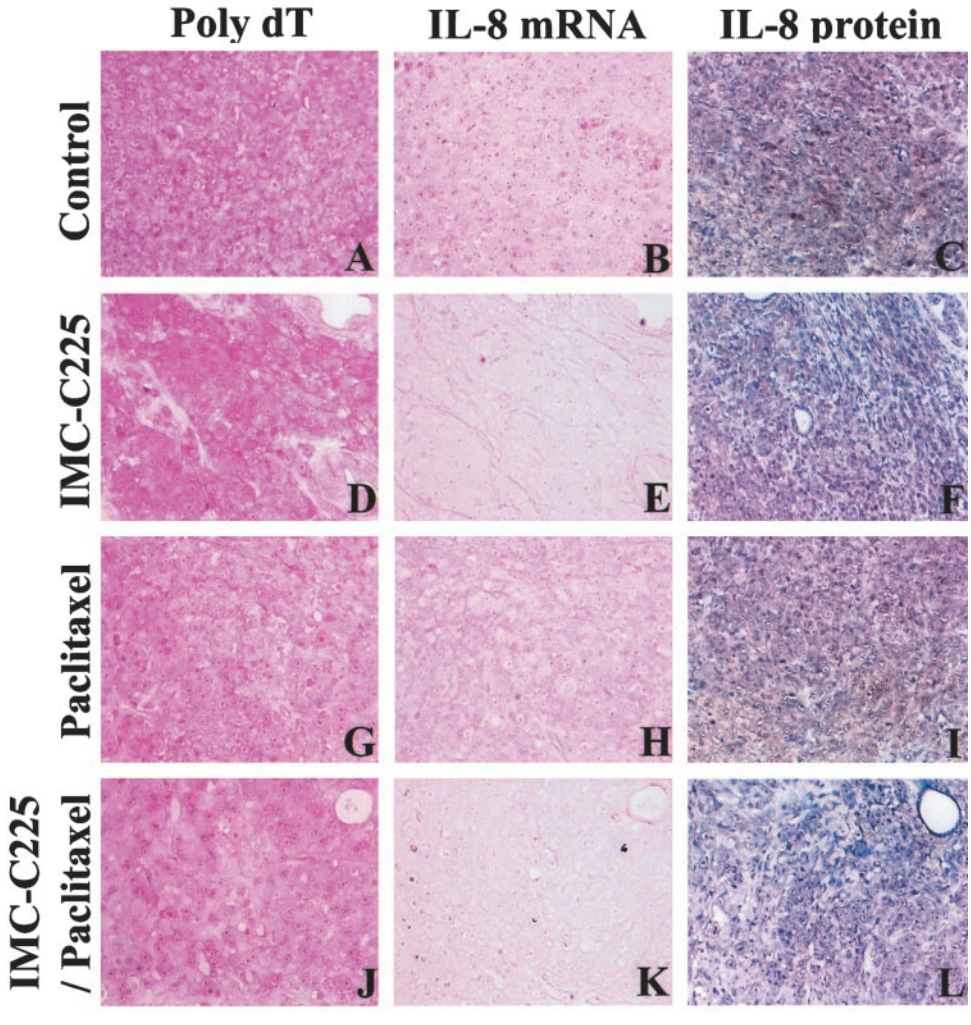


*Fig. 3* Down-regulation of IL-8 expression after IMC-C225 therapy in PC-3 M-LN4 xenografts growing in the prostate of athymic nude mice. Prostate tumors were harvested from saline-treated controls (*A–C*), IMC-C225 treated mice (*D–F*), paclitaxel-treated mice (*G–I*), and IMC-C225- plus paclitaxel-treated mice (*J–L*). The steady-state mRNA (*A, B, D, E, G, H, J,* and *K*) and protein (*C, F, I,* and *L*) expression of IL-8 was down-regulated in the tumors of mice treated with either IMC-C225 alone (*E* and *F*) or in combination with paclitaxel (*K* and *L*), compared with controls (*B and C*) or paclitaxel-treated mice (*H and I*). Poly(dT) (*A, D, G,* and *J*) served as control for mRNA integrity. All samples had an intense colorimetic reaction, indicating that the mRNA was well preserved.

(13). Treatment of the androgen-responsive MDA PCa 2a and MDA PCa 2b cell lines with flutamide and IMC-C225 decreased CDK2 activity and increased $p27^{kip1}$ to levels greater than that observed with IMC-C225 treatment alone (40). These studies suggest that the androgen-signaling pathway and growth factor-mediated pathway may coexist in the regulation of proliferation of PCa. In early stages of the progression of PCa, androgen is a dominant factor. After castration, growth factors

*Table 4* Apoptosis, proliferation, and MVD after therapy with IMC-C225 and/or paclitaxel

All therapy significantly inhibited proliferation and induced apoptosis of tumor cells compared with controls ($P < 0.05$). In particular, cell proliferation in the tumors treated with combination therapy with IMC-C225 and paclitaxel was significantly lower than in the tumor treated with paclitaxel alone ($P < 0.05$). The therapy with IMC-C225 significantly increased $p27^{kip1}$-positive cells compared with controls or paclitaxel alone ($P < 0.05$). MVD was significantly reduced in the tumor treated with either IMC-C225 and combination with paclitaxel ($P < 0.05$). Apoptosis of endothelial cells was significantly induced by IMC-C225 alone and combination therapy with IMC-C225 and paclitaxel compared with either controls or paclitaxel alone ($P < 0.05$).

| Therapy | Proliferation index[a] Mean ± SD | $p27^{kip1}$ index[a] Mean ± SD | Apoptosis index[a] Mean ± SD | MVD[b] Mean ± SD | Apoptosis index of endothelial cells[c] Mean ± SD |
|---|---|---|---|---|---|
| Control (saline) | 244 ± 55 | 9 ± 4 | 15 ± 4 | 76 ± 14 | 0.13 ± 0.26 |
| IMC-C225 | 164 ± 35[d] | 18 ± 5[d,f] | 24 ± 9[d] | 39 ± 17[d,f] | 0.88 ± 0.18[d,f] |
| Paclitaxel | 174 ± 43[d] | 10 ± 5 | 29 ± 8[d] | 74 ± 13 | 0.28 ± 0.21 |
| IMC-C225/paclitaxel | 139 ± 33[d,f] | 23 ± 11[d,f] | 30 ± 9[d] | 38 ± 5[d,f] | 1.36 ± 0.57[d,e,f] |

[a] The density of cell proliferation and $p27^{kip1}$ by immunohistochemistry with anti PCNA and $p27^{kip1}$ antibody, and tumor cell apoptosis by TUNEL assay was expressed as an average number of five highest areas identified within a single 100× field.

[b] Microvessel density was expressed as an average number of CD-31 + cells in the five highest areas identified within a single 100× field.

[c] The density of endothelial cell apoptosis by immunofluorescent CD-31 and TUNEL double labeling was expressed as an average of the ratio of apoptosis in the nucleus of endothelial cells to the total number of nuclei of endothelial cells taken from the areas with the highest MVD identified within a single 100× field.

[d] $P < 0.05$ compared to control.

[e] $P < 0.05$ compared to IMC-C225.

[f] $P < 0.05$ compared to paclitaxel ($P$: Mann-Whitney $U$ test).

may become a dominant factor to refuel the growth of PCa in an androgen-independent mechanism.

The anti-EGFR mAb IMC-225, which binds to the EGFR with a greater affinity than the natural ligands EGF or TGF-α, blocks the binding of EGF/TGF-α, and prevents activation of receptor tyrosine kinase (21–25). This antibody can inhibit the proliferation of a variety of malignant cell lines stimulated by either exogenous EGF or endogenous TGF-α (26–30) and has potent antitumor activity against a variety of cultured and human xenografts, principally through the induction of apoptosis and inhibition of invasion and tumor-induced angiogenesis (33–35, 38, 56). We reported previously that the *in vitro* treatment of bladder cancer with IMC-C225 resulted in only a modest antitumor effect, whereas *in vivo* therapy had profound effects on tumor growth, and both down-regulated the expression of the angiogenic factors VEGF, bFGF, IL-8, and MMP-9, and induced apoptosis of tumor and endothelial cells (33, 34). Previous reports indicate that IMC-C225 also inhibits the proliferation of the androgen-independent PCa cell lines DU145 and PC3 (37, 38, 40). In DU145 cells, the antibody-induced growth inhibition was associated with induction of the CDK inhibitor $p27^{kip1}$ (37), and regression of established DU145 xenografts, which overexpress the EGFR relative to PC-3M-LN4, was observed after therapy with IMC-C225 and doxorubicin (32). Furthermore, the direct injection of antisense oligonucleotides to TGF-α induced the regression of PC-3 xenografts in athymic nude mice (48).

The present study confirms that EGFR blockade with IMC-C225 inhibits the growth of the highly metastatic human PCa cell line PC-3M-LN4, which expresses relatively low levels of the EGFR compared with other PCa cell lines (32, 37, 40, 57). Therapy with IMC-C225 did not cause regression of PC-3M-LN4 as was reported previously for DU145 or A431 xenografts, which are profoundly dependent on EGFR signaling for their growth (31, 32). In the case of A431, therapy with EGFR inhibitors results in the complete regression of established tumors. However, when therapy is halted tumor regrowth occurs, which is resistant to additional EGFR-directed therapy. This acquired resistance is characterized by constitutive overexpression of VEGF (58). The PC-3M-LN4 tumor model is not ideal for these types of survival studies, because control animals succumb to tumor burden effects after 5–6 weeks, and the tumors in the treated animals do not regress completely.

Despite a minimal antiproliferative effect and lack of induction of $p27^{kip1}$ expression *in vitro*, therapy with IMC-C225 *in vivo* inhibited tumor cell proliferation, up-regulated $p27^{kip1}$ expression, enhanced tumor cell apoptosis, and down-regulated the expression of IL-8 (33, 34, 56). This activity was associated with endothelial cell apoptosis and the inhibition of tumor-induced angiogenesis, resulting in decreased tumor growth and metastatic tumor burden (33, 34, 56, 59). The antitumor effect observed with PC-3M-LN4 xenografts, which express low levels of EFGR (Fig. 1*A*), emphasizes that overexpression of the EGFR is not necessary for successful EGFR-directed therapy. Thus, any cell expressing even low levels of the EGFR represents a valid target. Indeed some of the therapeutic effects observed with IMC-C225 may be mediated by perturbations in the stromal-tumor interactions, perhaps via down-regulation of IL-8 as observed in the current study.

We hypothesize that IMC-C225 exerts its *in vivo* antitumor effect in androgen-independent PCa in part by down-regulating the expression of IL-8, which in turn induces endothelial cell apoptosis leading to the regression of tumor neovascularity. Inoue *et al.* (60) reported that metastatic PCa is characterized by an enhanced angiogenic response in the host microenvironment. Inoue *et al.* (60) also identified IL-8 as an important mediator of tumor-induced angiogenesis by the PC-3M-LN4 cell line, whereas VEGF was expressed at only low levels by this cell line (61). Down-regulation of IL-8 expression after stable transfection of PC-3M-LN4 with antisense IL-8 transcripts resulted in decreased tumor induced angiogenesis, tumorigenicity, and metastasis after implantation of the transfected cells into the pros-

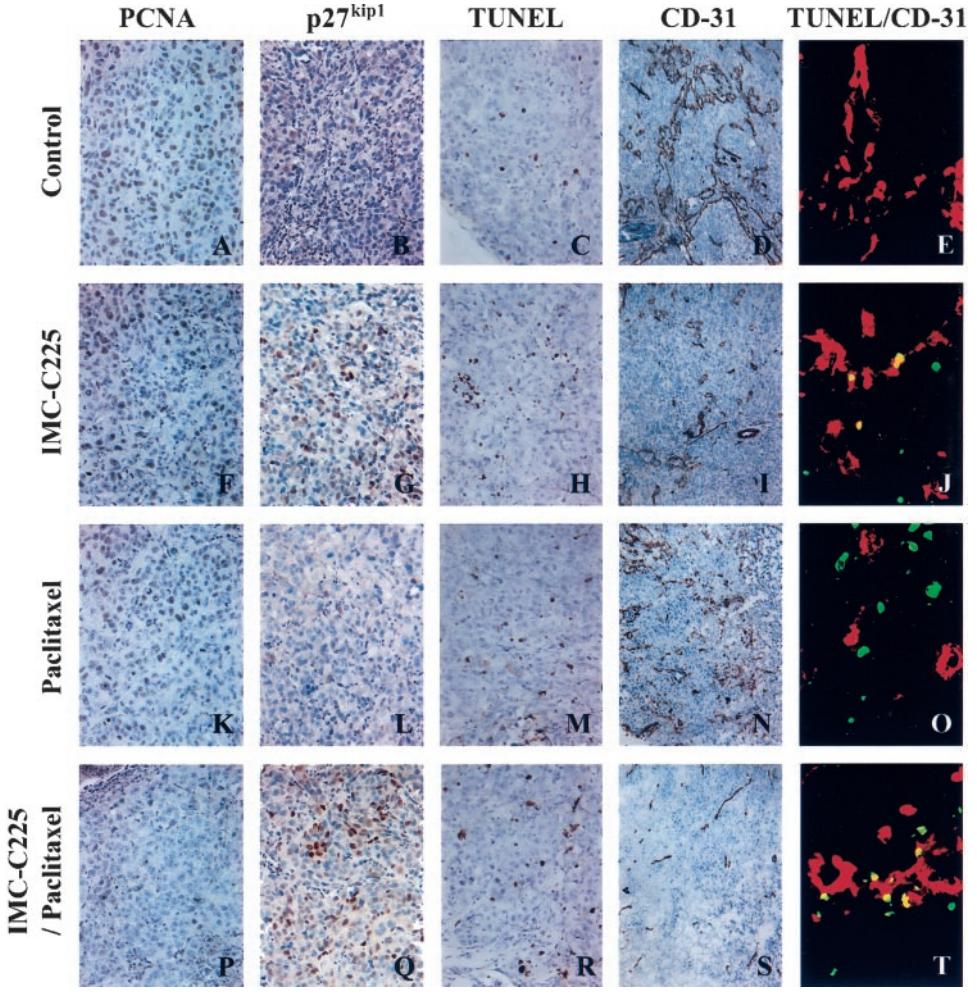


*Fig. 4* Immunohistochemical analysis of cellular proliferation (PCNA), expression of $p27^{kip1}$ apoptosis (TUNEL), MVD (CD-31), and double-staining immunofluorescence for endothelial cell apoptosis. Prostate tumors were harvested from saline-treated controls (*A–E*), IMC-C225-treated mice (*F–J*), paclitaxel-treated mice (*K–O*), and IMC-C225 plus paclitaxel-treated mice (*P–T*). Cellular proliferation was significantly reduced after IMC-C225 alone, paclitaxel alone, and IMC-C225 plus paclitaxel. The most significant inhibition in proliferation was seen after combination therapy with IMC-225 plus paclitaxel. The number of $p27^{kip1}$-positive cells was higher in the tumors of mice treated with IMC-C225, either alone or in combination with paclitaxel, compared with controls or paclitaxel-treated mice. By TUNEL analysis, apoptosis was enhanced after therapy, especially in the tumors of mice treated with IMC-C225 and paclitaxel combination. MVD was significantly reduced in the tumors of mice treated with IMC-C225, compared with saline controls or after paclitaxel therapy. Paclitaxel did not enhance the antiangiogenic effect of IMC-C225. Immunofluorescent double staining demonstrated tumor and endothelial cell apoptosis after therapy with the IMC-C225 and paclitaxel combination.

tate of athymic nude mice. These studies emphasize the importance of IL-8 as a mediator of the angiogenic response induced by PC-3M-LN4 and support the hypothesis therapy such as anti-EGFR therapy, which targets IL-8 expression may be effective against androgen-independent PCa. Similar observations were made after the successful treatment of human bladder and pancreatic cancer xenografts in nude mice (33, 34, 56). Collectively, these studies demonstrate that down-regulation of the angiogenic stimulus provided by the tumor cells inhibits the host angiogenic response and emphasize the complexity of tumor-host interactions. The enhanced induction of tumor and endothelial cell apoptosis after therapy with IMC-C225 and paclitaxel may be because of the dependence these cells on IL-8 as a survival factor after cellular damage from paclitaxel therapy, tipping the balance toward drug-induced apoptosis. This is consistent with the role of IL-8 as survival factors in ovarian cancer after therapy with paclitaxel or other chemotherapeutic agents (62, 63). The present study demonstrates that inhibition of angiogenesis characterizes, in part, the antitumor effect of EGFR blockade in PCa, and confirms the importance of IL-8 as a mediator of PCa angiogenesis and metastasis (18, 60, 64, 65).

The antitumor activity of IMC-C225 against PCa xenografts was enhanced by the simultaneous administration of systemic paclitaxel similar to results observed after the treatment of human bladder cancer (34). Paclitaxel was used in these studies because it demonstrates significant antitumor effect against PCa, both as a single agent and in combination with other cytotoxic agents (41, 42). Paclitaxel also mediates a direct antiangiogenic effect against several cell lines but did not exert this effect against PC-3M-LN4. The reason for minimum effects

of paclitaxel might be that the development of drug resistance by exposure to paclitaxel was accompanied with alterations of gene expression including IL-8 (63). Paclitaxel increases microtubule stability by preventing tubulin depolymerization, which results in tubulin bundling (66, 67). These cytoskeleton changes lead to cell cycle arrest and apoptosis within 20 h of paclitaxel exposure (45, 46). On the other hand, the induction of $G_1$ arrest by IMC-C225 is associated with the inhibition of CDK-2 activity and increased levels of the CDK inhibitor $p27^{kip1}$ (40). In fact, IMC-C225 augments the antitumor activity of several chemotherapeutic agents and irradiation in human xenograft models (30, 32, 34, 56, 68, 69). The molecular pathways for this effect are unclear, but the effect may be mediated by several different mechanisms including DNA repair (70), multidrug resistance (71, 72), cell cycle checkpoint control (73), or angiogenesis (33, 34, 56, 59). The capacity of IMC-C225 to modulate cell cycle distribution may also play a central role in regulating the increased sensitivity to chemotherapeutic agents and irradiation. This may involve cell cycle checkpoint control as an activator of cell death (73). EGFR blockade results in cellular arrest at the $G_1$ restriction point, and cells typically damaged by chemotherapy typically arrest in $G_2$-M to repair DNA alterations. Mendelsohn (73) hypothesized that tumor cells die if they consecutively ignore two checkpoint signals activated by EGFR blockade and cytotoxic chemotherapy. In contrast, nonmalignant epithelial cells that obey checkpoint control signals may be less susceptible to the cytotoxic effects of these combination treatments.

In summary our experiments demonstrate that paclitaxel enhances the antitumor effect of IMC-C225 for the therapy of human androgen-independent PCa growing within the prostate gland of athymic nude mice and demonstrate the benefit of combining two therapeutic modalities that have entirely different mechanisms of activity. The results of this preclinical study justify the clinical application of this form of combination therapy for the treatment of metastatic PCa.

## REFERENCES

1. Greenlee, R. T., Murray, T., Bolden, S., and Wingo, P. A. Cancer statistics, 2000. CA Cancer J. Clin., *50:* 7–33, 2000.

2. Catalona, W. J. Management of cancer of the prostate. N. Engl. J. Med., *331:* 996–1004, 1994.

3. Kreis, W. Current chemotherapy and future directions in research for the treatment of advanced hormone-refractory prostate cancer. Cancer Investig., *13:* 296–231, 1995.

4. Panvichian, R., and Pienta, K. J. Hormonal and chemotherapeutic systemic therapy for metastatic prostate cancer. Cancer Control, *3:* 493–500, 1996.

5. Culig, Z., Hobisch, A., Cronauer, M. V., Radmayr, C., Hittmair, A., Zhang, J., Thurnher, M., Bartsch, G., and Klocker, H. Regulation of prostatic growth and function by peptide growth factors. Prostate, *28:* 392–405, 1996.

6. Motta, M., Dondi, D., Moretti, R. M., Montagnani, M. M., Pimpinelli, F., Maggi, R., and Limonta, P. Role of growth factors, steroid and peptide hormones in the regulation of human prostatic tumor growth. J. Steroid Biochem. Mol. Biol., *56:* 107–111, 1996.

7. Dondi, D., Moretti, R. M., Marelli, M. M., Motta, M., and Limonta, P. Growth factors in steroid-responsive prostatic tumor cells. Steroids, *61:* 222–225, 1996.

8. Sherwood, E. R., and Lee, C. Epidermal growth factor-related peptides and the epidermal growth factor receptor in normal and malignant prostate. World J. Urol., *13:* 290–296, 1995.

9. Limonta, P., Dondi, D., Marelli, M. M., Moretti, R. M., Negri-Cesi, P., and Motta, M. Growth of the androgen-dependent tumor of the prostate: role of androgens and of locally expressed growth modulatory factors. J. Steroid Biochem. Mol. Biol., *53:* 401–405, 1995.

10. Connolly, J. M., and Rose, D. P. Regulation of DU145 human prostate cancer cell proliferation by insulin-like growth factors and its interaction with the epidermal growth factor autocrine loop. Prostate, *24:* 167–175, 1994.

11. Habib, F. K., and Chisholm, G. D. The role of growth factors in the human prostate. Scand. J. Urol. Nephrol. Suppl., *138:* 53–58, 1991.

12. Chan, J. M., Stampfer, M. J., Giovannucci, E., Gann, P. H., Ma, J., Wilkinson, P., Hennekens, C. H., and Pollak, M. Plasma insulin-like growth factor-I and prostate cancer risk: a prospective study. Science (Wash. DC), *279:* 563–566, 1998.

13. Culig, Z., Hobisch, A., Cronauer, M. V., Radmayr, C., Trapman, J., Hittmair, A., Bartsch, G., and Klocker, H. Androgen receptor activation in prostatic tumor cell lines by insulin-like growth factor-I, keratinocyte growth factor, and epidermal growth factor. Cancer Res., *54:* 5474–5478, 1994.

14. Connolly, J. M., and Rose, D. P. Angiogenesis in two human prostate cancer cell lines with differing metastatic potential when growing as solid tumors in nude mice. J. Urol., *160:* 932–936, 1998.

15. Wikstrom, P., Stattin, P., Franck-Lissbrant, I., Damber, J. E., and Bergh, A. Transforming growth factor β1 is associated with angiogenesis, metastasis, and poor clinical outcome in prostate cancer. Prostate, *37:* 19–29, 1998.

16. Campbell, S. C. Advances in angiogenesis research: relevance to urological oncology. J. Urol., *158:* 1663–1674, 1997.

17. Horan, A. H. Re: Advances in angiogenesis research: relevance to urological oncology. J. Urol., *160:* 134–135, 1998.

18. Greene, G. F., Kitadai, Y., Pettaway, C. A., von Eschenbach, A. C., Bucana, C. D., and Fidler, I. J. Correlation of metastasis-related gene expression with metastatic potential in human prostate carcinoma cells implanted in nude mice using an *in situ* messenger RNA hybridization technique. Am. J. Pathol., *150:* 1571–1582, 1997.

19. Fidler, I. J., Kumar, R., Bielenberg, D. R., and Ellis, L. M. Molecular determinants of angiogenesis in cancer metastasis. Cancer J. Sci. Am. S58–S66, 1998.

20. Folkman, J. Tumor angiogenesis. Adv. Cancer Res., *43:* 175–203, 1985.

21. Sato, J. D., Kawamoto, T., Le, A. D., Mendelsohn, J., Polikoff, J., and Sato, G. H. Biological effects *in vitro* of monoclonal antibodies to human epidermal growth factor receptors. Mol. Biol. Med., *1:* 511–529, 1983.

22. Kawamoto, T., Sato, J. D., Le, A., Polikoff, J., Sato, G. H., and Mendelsohn, J. Growth stimulation of A431 cells by epidermal growth factor: identification of high-affinity receptors for epidermal growth factor by an anti-receptor monoclonal antibody. Proc. Natl. Acad. Sci. USA, *80:* 1337–1341, 1983.

23. Kawamoto, T., Mendelsohn, J., Le, A., Sato, G. H., Lazar, C. S., and Gill, G. N. Relation of epidermal growth factor receptor concentration to growth of human epidermoid carcinoma A431 cells. J. Biol. Chem., *259:* 7761–7766, 1984.

24. Fan, Z., Lu, Y., Wu, X., and Mendelsohn, J. Antibody-induced epidermal growth factor receptor dimerization mediates inhibition of autocrine proliferation of A431 squamous carcinoma cells. J. Biol. Chem., *269:* 27595–27602, 1994.

25. Fan, Z., Masui, H., Altas, I., and Mendelsohn, J. Blockade of epidermal growth factor receptor function by bivalent and monovalent fragments of 225 anti-epidermal growth factor receptor monoclonal antibodies. Cancer Res., *53:* 4322–4328, 1993.

26. Mendelsohn, J. Epidermal growth factor receptor as a target for therapy with antireceptor monoclonal antibodies. J. Natl. Cancer Inst. Monogr., 125–131, 1992.

27. Masui, H., Moroyama, T., and Mendelsohn, J. Mechanism of antitumor activity in mice for anti-epidermal growth factor receptor monoclonal antibodies with different isotypes. Cancer Res., *46:* 5592–5598, 1986.

28. Masui, H., Kawamoto, T., Sato, J. D., Wolf, B., Sato, G., and Mendelsohn, J. Growth inhibition of human tumor cells in athymic mice by anti-epidermal growth factor receptor monoclonal antibodies. Cancer Res., *44:* 1002–1007, 1984.

29. Fan, Z., Baselga, J., Masui, H., and Mendelsohn, J. Antitumor effect of anti-epidermal growth factor receptor monoclonal antibodies plus *cis*-diamminedichloroplatinum on well established A431 cell xenografts. Cancer Res., *53:* 4637–4642, 1993.

30. Baselga, J., Norton, L., Masui, H., Pandiella, A., Coplan, K., Miller, W. J., and Mendelsohn, J. Antitumor effects of doxorubicin in combination with anti-epidermal growth factor receptor monoclonal antibodies. J. Natl. Cancer Inst., *85:* 1327–1333, 1993.

31. Goldstein, N. I., Prewett, M., Zuklys, K., Rockwell, P., and Mendelsohn, J. Biological efficacy of a chimeric antibody to the epidermal growth factor receptor in a human tumor xenograft model. Clin. Cancer Res., *1:* 1311–1318, 1995.

32. Prewett, M., Rockwell, P., Rockwell, R. F., Giorgio, N. A., Mendelsohn, J., Scher, H. I., and Goldstein, N. I. The biologic effects of C225, a chimeric monoclonal antibody to the EGFR, on human prostate carcinoma. J. Immunother. Emphas. Tumor Immunol., *19:* 419–427, 1996.

33. Perrotte, P., Matsumoto, T., Inoue, K., Kuniyasu, H., Eve, B. Y., Hicklin, D. J., Radinsky, R., and Dinney, C. P. N. Anti-epidermal growth factor receptor antibody C225 inhibits angiogenesis in human transitional cell carcinoma growing orthotopically in nude mice. Clin. Cancer Res., *5:* 257–264, 1999.

34. Inoue, K, Slaton, J. W., Perrotte, P., Davis, D. W., Bruns, C. J., Hicklin, D. J., McConkey, D. J., Sweeney, P., Radinsky, R., and Dinney, C. P. N. Paclitaxel enhances the effects of the anti-epidermal growth factor receptor monoclonal antibody ImClone C225 in mice with metastatic human bladder transitional cell carcinoma. Clin. Cancer Res., *6:* 4874–4884, 2000.

35. Putz, T., Culig, Z., Eder, I. E., Nessler-Menardi, C., Bartsch, G., Grunicke, H., Uberall, F., and Klocker, H. Epidermal growth factor (EGF) receptor blockade inhibits the action of EGF, insulin-like growth factor I, and a protein kinase A activator on the mitogen-activated protein kinase pathway in prostate cancer cell lines. Cancer Res., *59:* 227–233, 1999.

36. Connolly, J. M., and Rose, D. P. Autocrine regulation of DU145 human prostate cancer cell growth by epidermal growth factor-related polypeptides. Prostate, *19:* 173–180, 1991.

37. Peng, D., Fan, Z., Lu, Y., DeBlasio, T., Scher, H., and Mendelsohn, J. Anti-epidermal growth factor receptor monoclonal antibody 225 upregulates $p27^{kip1}$ and induces $G_1$ arrest in prostatic cancer cell line DU145. Cancer Res., *56:* 3666–3669, 1996.

38. Fong, C. J., Sherwood, E. R., Mendelsohn, J., Lee, C., and Kozlowski, J. M. Epidermal growth factor receptor monoclonal antibody inhibits constitutive receptor phosphorylation, reduces autonomous growth, and sensitizes androgen-independent prostatic carcinoma cells to tumor necrosis factor α. Cancer Res., *52:* 5887–5892, 1992.

39. Hofer, D. R., Sherwood, E. R., Bromberg, W. D., Mendelsohn, J., Lee, C., and Kozlowski, J. M. Autonomous growth of androgen-independent human prostatic carcinoma cells: role of transforming growth factor α. Cancer Res., *51:* 2780–2785, 1991.

40. Ye, D., Mendelsohn, J., and Fan, Z. Androgen and epidermal growth factor down-regulate cyclin-dependent kinase inhibitor $p27^{kip1}$Kipl and costimulate proliferation of MDA PCa 2a and MDA PCa 2b prostate cancer cells. Clin. Cancer Res., *5:* 2171–2177, 1999.

41. Hudes, G. R., Nathan, F. E., Khater, C., Greenberg, R., Gomella, L., Stern, C., and McAlee, C. Paclitaxel plus estramustine in metastatic hormone-refractory prostate cancer. Semin. Oncol., *22:* 41–55, 1995.

42. Pienta, K. J., and Smith, D. C. Paclitaxel, estramustine, and etoposide in the treatment of hormone-refractory prostate cancer. Semin. Oncol., *24:* S15-72–S15-77, 1997.

43. Pettaway, C. A., Pathak, S., Greene, G., Ramirez, E., Wilson, M. R., Killion, J. J., and Fidler, I. J. Selection of highly metastatic variants of different human prostatic carcinomas using orthotopic implantation in nude mice. Clin. Cancer Res., *2:* 1627–1636, 1996.

44. Mosmann, T. Rapid colorimetic assay for cellular growth and survival: application to proliferation and cytotoxicity assays. J. Immunol. Methods, *65:* 55–63, 1983.

45. Kitadai, Y., Bucana, C. D., Ellis, L. M., Anzai, H., Tahara, E., and Fidler, I. J. *In situ* mRNA hybridization technique for analysis of metastasis-related genes in human colon carcinoma cells. Am. J. Pathol., *147:* 1238–1247, 1995.

46. Radinsky, R., Bucana, C. D., Ellis, L. M., Sanchez, R., Cleary, K. R., Brigati, D. J., and Fidler, I. J. A rapid colorimetric *in situ* messenger RNA hybridization technique for analysis of epidermal growth factor receptor in paraffin-embedded surgical specimens of human colon carcinomas. Cancer Res., *53:* 937–943, 1993.

47. Vecchi, A., Garlanda, C., Lampugnani, M. G., Resnati, M., Matteucci, C., Stoppacciaro, A., Schnurch, H., Risau, W., Ruco, L., Mantovani, A., and Dejana, E. Monoclonal antibodies specific for endothelial cells of mouse blood vessels. Their application in the identification of adult and embryonic endothelium, Eur. J. Cell Biol., *63:* 247–254, 1994.

48. Weidner, N., Semple, J. P., Welch, W. R., and Folkman, J. Tumor angiogenesis and metastasis–correlation in invasive breast carcinoma. N. Engl. J. Med., *324:* 1–8, 1991.

49. Fan, Z., Shang, B. Y., Lu, Y., Chou, J-L., and Mendelsohn, J. Reciprocal changes in $p27^{kip1}$ and $p21^{Cip1}$ in growth inhibition mediated by blockade or overstimulation of epidermal growth factor receptors. Clin. Cancer Res., *3:* 1943–1948, 1997.

50. Rubenstein, M., Mirochnik, Y., Chou, P., Guinan, P. Growth factor deprivation therapy of hormone insensitive prostate and breast cancers utilizing antisense oligonucleotides. Methods Find. Exp. Clin. Pharmacol., *20:* 825–831, 1998.

51. Scher, H. I., Sarkis, A., Reuter, V., Cohen, D., Netto, G., Petrylak, D., Lianes, P., Fuks, Z., Mendelsohn, J., and Cordon-Cardo, C. Changing pattern of expression of the epidermal growth factor receptor and transforming growth factor α in the progression of prostatic neoplasms. Clin. Cancer Res., *1:* 545–550, 1995.

52. Sherwood, E. R., Van Dongen, J. L., Wood, C. G., Liao, S., Kozlowski, J. M., and Lee, C. Epidermal growth factor receptor activation in androgen-independent but not androgen-stimulated growth of human prostatic carcinoma cells. Br. J. Cancer, *77:* 855–861, 1998.

53. Gioeli, D., Mandell, J. W., Petroni, G. R., Frierson, H. J., and Weber, M. J. Activation of mitogen-activated protein kinase associated with prostate cancer progression. Cancer Res., *59:* 279–284, 1999.

54. Myers, R. B., Kudlow, J. E., and Grizzle, W. E. Expression of transforming growth factor-α, epidermal growth factor and the epidermal growth factor receptor in adenocarcinoma of the prostate and benign prostatic hyperplasia. Mod. Pathol., *6:* 733–737, 1993.

55. Liu, X. H., Wiley, H. S., and Meikle, A. W. Androgens regulate proliferation of human prostate cancer cells in culture by increasing transforming growth factor-α (TGF-α) and epidermal growth factor (EGF)/TGF-α receptor. J. Clin. Endocrinol. Metab., *77:* 1472–1478, 1993.

56. Ching, K. Z., Ramsey, E., Pettigrew, N., D'Cunha, R., Jason, M., and Dodd, J. G. Expression of mRNA for epidermal growth factor, transforming growth factor-α and their receptor in human prostate tissue and cell lines. Mol. Cell Biochem., *126:* 151–158, 1993.

57. Bruns, C. J., Harbison, M. T., Davis, D. W., Portera, C. A., Tsan, R., McConkey, D. J., Evans, D. B., Abbruzzese, J. L., Hicklin, D. J., and Radinsky, R. Epidermal growth factor receptor blockade with C225 plus gemcitabine results in regression of human pancreatic carcinoma growing orthotopically in nude mice by antiangiogenic mechanisms. Clin. Cancer Res., *6:* 1936–1948, 2000.

58. Viloria-Petit, A., Crombet, T., Jothy, S., Hicklin, D., Bohlen, P., Schlaeppi, J. M., Rak, J., and Kerbel, R. S. Acquired resistance to the antitumor effect of epidermal growth factor receptor-blocking antibod-

ies *in vivo*: a role for altered tumor angiogenesis. Cancer Res., *61:* 5090–5101, 2001.

59. Petit, A. M., Rak, V., Hung, W. C., Rockwell, P., Goldstein, N., Fendly, B., and Kerbel, R. S. Neutralizing antibodies against epidermal growth factor and ErbB-2/neu receptor tyrosine kinases down-regulate vascular endothelial growth factor production by tumor cells *in vitro* and *in vivo*: angiogenic implications for signal transduction therapy of solid tumors. Am. J. Pathol., *151:* 1523–1530, 1997.

60. Inoue, K., Slaton, J. W., Eve, B. Y., Kim, S. J., Perrotte, P., Balbay, M. D., Yano, S., Bar-Eli, M., Radinsky, R., Pettaway, C. A., and Dinney, C. P. Interleukin 8 expression regulates tumorigenicity and metastases in androgen-independent prostate cancer. Clin. Cancer Res., *6:* 2104–2119, 2000.

61. Balbay, M. D., Pettaway, C. A., Kuniyasu, H., Ramirez, E., Li, E., Fidler, I. J., and Dinney, C. P. Highly metastatic human prostate cancer growing within the prostate of athymic nude mice overexpresses vascular endothelial growth factor. Clin. Can. Res., *5:* 783–789, 1999.

62. Lee, L. F., Schuerer-Maly, C. C., Lofquist, A. K., van Haaften-Day, C., Ting, J. P., White, C. M., Martin, B. K., and Haskill, J. S. Taxol-dependent transcriptional activation of Il-8 expression in a subset of human ovarian cancer. Cancer Res., *56:* 1303–1308, 1996.

63. Duan, Z., Feller, A. J., Penson, R. T., Chabner, B. A., and Seiden, M. V. Discovery of differentially expressed genes associated with paclitaxel resistance using cDNA array technology: analysis of interleukin (IL) 6, IL-8, and monocyte chemotactic protein 1 in the paclitaxel-resistant phenotype. Clin. Cancer Res., *5:* 3445–3453, 1999.

64. Veltri R. W., Miller, M. C., Zhao, G., Ng, A., Marley, G. M., Wright, G. L., Jr., Vessell, R. L., and Ralph, D. Interleukin-8 serum levels in patients with benign prostatic hyperplasia and prostate cancer. Urology, *53:* 139–147, 1999.

65. Moore, B. B., Arenberg, D. A., Stoy, K., Morgan, T., Addison, C. L., Morris, S. D., Glass, M., Wilke, C., Xue, Y. Y., Sitterding, S., Kunkel, S. L., Burdick. M. D., and Strieter, R. M. Distinct CXC chemokines mediate tumorigenicity of prostate cancer cells. Am. J. Pathol., *154:* 1503–1512, 1999.

66. Horwitz, S. B. Mechanism of action of taxol. Trends Pharmacol. Sci., *13:* 134–136, 1992.

67. Rowinsky, E. K., Cazenave, L. A., and Donehower, R. C. Taxol: a novel investigational antimicrotubule agent. J. Natl. Cancer Inst., *82:* 1247–1259, 1990.

68. Huang, S-M., Bock, J. M., and Harari, P. M. Epidermal growth factor receptor blockade with c225 modulates proliferation, apoptosis, and radiosensitivity in squamous cell carcinomas of the head and neck. Cancer Res., *59:* 1935–1940, 1999.

69. van Gog, F. D., Brakenhoff, R. H., Stigter-van Walsum, M., Snow, G. B., and van Dongen, G. A. Perspectives of combined radioimmunotherapy and anti-EGFR antibody therapy for the treatment of residual head and neck cancer. Int. J. Cancer, *77:* 13–18, 1998.

70. Bandyopadkyay, D., Mandal, M., Adam, L., Mendelsohn, J., and Kumar, R. Physical interaction between epidermal growth factor receptor and DNA-dependent protein kinase in mammalian cells. J. Biol. Chem., *273:* 1568–1573, 1998.

71. Meyers, M. B, Merluzzi, V. J., Spengler, B. A., and Biedler, J. L. Epidermal growth factor receptor is increased in multidrug-resistant Chinese hamster and mouse tumor cells. Proc. Natl. Acad. Sci. USA, *83:* 5521–5525, 1986.

72. Nagane, M., Levitzki, A., Gazit, A., Cavenee, W. K., and Huang, H. J. Drug resistance of human glioblastoma cells conferred by a tumor-specific mutant epidermal growth factor receptor through modulation of Bcl-XL and caspase-3-like proteases. Proc. Natl. Acad. Sc. USA, *95:* 5724–5729, 1998.

73. Mendelsohn, J. Epidermal growth factor receptor inhibition by a monoclonal antibody as anticancer therapy. Clin. Cancer Res., *3:* 2703–2707, 1997.